

Post-print author

180° pinhole-SPECT with tilted detector and OS-EM reconstruction: phantom studies and potential clinical applications

Alain Seret¹, Michel Defrise² and Didier Blocklet³.

¹Université de Liège (ULg), Imagerie médicale expérimentale, Liège, Belgium

²Vrije Universiteit Brussel (VUB), Division of Nuclear Medicine, Brussels, Belgium

³Université Libre de Bruxelles (ULB), Hopital Erasme, Radioisotopes, Brussels,
Belgium.

Corresponding author: Alain Seret, Université de Liège (ULg), Imagerie médicale
expérimentale, Institut de Physique, B5, B-4000 Liège1, Belgium

Phone 32-4-3663705; Fax 32-4-3662813, e-mail aseret@ulg.ac.be

Reprint request: Alain Seret, Université de Liège (ULg), Imagerie médicale
expérimentale, Institut de Physique, B5, B-4000 Liège1, Belgium,

e-mail aseret@ulg.ac.be

Abstract

This study investigated the feasibility of OS-EM reconstruction of pinhole SPECT acquired with a tilted detector head and a 180° orbit. Phantom and patient data have been recorded using a standard single head camera. Reconstructions have been performed using a dedicated OS-EM algorithm. Reconstructed images of line, uniformity and Picker's thyroid phantoms showed that the geometry, the physical size and the uniformity of the radioactive objects are preserved. For the range of radius corresponding to the patient studies, the measured full widths at half-maximum lie between (4.90 ± 0.25) mm and (6.05 ± 0.25) mm. Finally the gain in resolution associated with the use of the pinhole collimator instead of a parallel hole collimator is highlighted in a parathyroid exploration and in a shoulder bone study.

Keywords: pinhole, SPECT, pinhole-SPECT, OSEM

INTRODUCTION

Pinhole collimators (PH) allow extrinsic resolution below the nominal intrinsic resolution of the gamma camera [1]. However, the field of view is strongly limited and depends on the distance between the collimator and the target. Therefore, the clinical use of pinhole collimated cameras is limited in humans to a few areas, namely the neck and some joints [2-4]. With the recent developments of three-dimensional tomographic reconstruction algorithms for non-parallel geometries [5], pinhole single photon emission tomography (PH SPECT) has become practical [1, 2, 4, 6-11]. Mainly applied to small animal studies (a review of these works can be found in [8]), PH SPECT was also shown to be clinically relevant for human imaging [2-4, 10, 11]. For the small animals as well as for some human joints (foot, knee, wrist) a full 360° orbit appears satisfactory. However for the shoulder joint and for the neck, only a limited 180° orbit would be practicable. Moreover, in the thyroid area, the detector has to be tilted in order to minimize the orbit radius [2].

In the recent years, it has been shown that the ML-EM algorithm [1, 11] and its accelerated version OS-EM [9] offer to PH SPECT the same benefits compared to the filtered backprojection (FBP) as to the parallel geometry : there is a global gain in overall image quality, especially in the case of noisy data, resolution and uniformity are improved and most of the geometrical distortions are eliminated. However, these studies were limited to a full 360° orbit or a 180° orbit without tilt.

We present here the study of PH OS-EM in the case of acquisitions with 180° circular orbit and with a tilted detector. Different phantoms have been used to evaluate both the achievable resolution and uniformity and the possibility of measuring accurately distances on the reconstructed images. Two clinical cases are then reported. One is the use of PH SPECT for shoulder bone SPECT and illustrates

Post-print author

the application of a 180° orbit PH SPECT without tilt. The other is a parathyroid exploration and illustrates the application of 180° orbit PH SPECT with a tilt. In both cases, SPECT with an ultra high resolution parallel hole collimator (UHR SPECT) has also been recorded and reconstructed with OS-EM for parallel geometry in order to evaluate the clinical improvement that could be expected from the combined use of PH SPECT and PH OS-EM.

MATERIALS AND METHODS

Camera and collimators

A Sophy DSX camera (SMV International, Buc, France) was used for all SPECT acquisitions. The pinhole collimator had a height of 205 mm and a circular base diameter of 295 mm. Using data obtained from SMV, the following relation between the pinhole radius (PR) and the detector radius (DR) could be established (Fig 1a):

$$\text{PR (in mm)} = \text{DR (in mm)} - 209.2 \cos(\text{tilt angle}). \quad (1)$$

UHR SPECT was performed with a low-energy ultra high resolution (SMV LE-THR 6.5-140) collimator.

Common acquisition and reconstruction parameters

With the exception of the uniformity phantom, phantoms and patients were positioned in order to get the area to be imaged within the half cylinder delimited by the rotation orbit and the plane passing through the orbit extremities and orthogonal to the orbit plane (Fig 1b). This condition is necessary to get sufficient projection data for accurate reconstruction in the plane of the PH orbit [5]. Outside this central plane, accurate cone-beam reconstruction is impossible, even with a 360° circular orbit. Therefore increasing artifacts should be expected in planes located at an increasing distance from the central plane. The energy window was centered at 140 keV with a total width of 20 %. With both collimators, 32 projections (128*128 images) per 180° of orbit were acquired. For the phantoms, 0° and 20° tilt angles were used with a hardware zoom of 2.0. The other parameters varied with the type of acquisition.

The PH OS-EM algorithm is a straightforward implementation [9] of the OSEM method [12] for the PH geometry, using simple voxel-driven backprojector

and ray-driven forward-projector that do not model the finite dimension of the pinhole aperture. OS-EM for parallel geometry was performed using the algorithm of the Vision nuclear medicine software (releases 4.2.1 and 5.1.0, SMV international, Buc, France). OSEM reconstructions were always performed with 8 subsets and 2 iterations. They resulted in 128 128*128 transverse slices. Slice pixel size and slice thickness can be freely chosen for PH OS-EM. For UHR SPECT OS-EM, the SMV Vision software does not offer this opportunity. Therefore, the slice pixel size and the slice thickness are equal to $(4.45/\text{zoom})$ mm. No attempt to correct for attenuation, scatter or resolution was made. When explicitly mentioned and for the patient studies only, the reconstructed PH-SPECT slices have been filtered with the gaussian filter of the Vision software.

Line source and uniformity phantoms

Two capillary tubes were filled with an aqueous solution of Tc99m. One tube was positioned along (within 1 cm) the axis of rotation and the second was located parallel to and at (23.3 ± 0.5) mm from this first line ((20.0 ± 0.5) mm horizontally and (12 ± 0.5) mm vertically). A 250 ml laboratory bottle of 5.8 cm inner diameter filled with an aqueous solution of 375 MBq Tc99m served as uniformity phantom. It was positioned with its cylindrical axis parallel and close (within 5 mm) to the axis of rotation. PH 360° SPECT with the 5 mm pinhole aperture was performed. A mean of 275 kcounts per projection without tilt and of 224 kcounts per projection with the 20° tilt angle were accumulated. Acquisitions with a 180° orbit have been extracted from the 360° orbit data. Data were reconstructed with a pixel size and a slice thickness equal to 0.25 mm for the line phantom and to 1.0 mm for the uniformity phantom. Full width at half maximum (FWHM) was measured on count density profiles obtained from the reconstructed line source phantom. The distance between the two

lines was also obtained from the count density profiles and taken as the distance between the two profile maxima. The error on both FWHMs and distances between the lines is one pixel or 0.25 mm. A region of interest (ROI) of 4.6 cm diameter was drawn on 10 reconstructed slices of the uniformity phantom. The standard deviation (rms) of the reconstructed pixel values in this ROI was calculated for each slice and the average (± 1 standard deviation) of the 10 rms calculated in this way was used as uniformity index. The diameter of the ROI corresponded to the inner diameter of the phantom (5.8 cm) minus two times the largest FWHM determined from the line source experiments (see Results and Table 1).

Picker's thyroid phantom

After being filled with an aqueous solution of 375 MBq Tc99m, the Picker thyroid phantom [9] was positioned just above the axis of rotation in order to mimick the physiological conditions that can be used for patient studies. 180° PH SPECT (right lateral to left lateral) was performed with the 3 mm pinhole aperture. A mean of 240 kcounts per projection was accumulated. The rotation radius was adapted to get PR = 75 mm for both tilt angles. Data were reconstructed with pixel size and slice thickness of 1.0 mm.

Parathyroid patient.

This patient was a 70 year-old women with primary hyperparathyroidism. 10-min pinhole planar images were acquired 10 min and 2 hours after the injection of 930 MBq 99mTc-methoxyisobutylisonitrile (MIBI) following the single tracer method. Between these two planar acquisitions, anterior 180° UHR SPECT (50 s per projection) and then anterior 180° PH SPECT (45 s per projection) have been performed. The pinhole aperture was 5 mm and the tilt angle was 20°. The pixel size and the slice thickness were equal to 1 mm for PH OS-EM. For the sake of

comparison, the volume reconstructed from UHR SPECT was zoomed to obtain the same pixel size and the same slice thickness. Since the scintigraphic exploration, this patient was not operated on. However, hyperparathyroidism remained.

Shoulder patient

This patient was a 55 year-old women with a left shoulder pain associated to a corticosteroid-induced osteoporosis. Three hours after injection of 750 MBq ^{99m}Tc -methylene diphosphonate (MDP), a classical whole body scan was performed followed by static spots and then left lateral 180° UHR SPECT. Projections of 30 s were obtained in 64*64 with a hardware zoom of 1.6. A 180° PH SPECT (45 s per projection) followed immediately with a pinhole aperture of 5 mm and without tilt.

RESULTS

Sagittal, coronal and oblique slices of the reconstructed line source phantom showed always perfectly linear and parallel lines. Moreover streak artifacts were not observed on any slice. For each acquisition orbit and each tilt angle, almost identical results were obtained for the 360° and 180° orbits. The results are gathered in Table 1. For the sake of comparisons, different orbits have been used for the acquisitions with and without tilt. Because PR and DR could not be both kept constant (see eq 1), DR was fixed at 270 mm for the smallest orbit and PR was fixed at 110 mm for the largest orbit. With the tilt, these 2 orbits are representative of orbits adopted with patients for the neck area. The largest orbit without tilt is close to the orbit used for the shoulder clinical case presented below.

Transverse slices of the reconstructed uniformity phantom are displayed in Fig. 2. Without tilt, the rms amounts to $(18.9 \pm 1.5)\%$ for the 360° orbit and to $(19.2 \pm 1.8)\%$ for the 180° orbit. With a tilt angle of 20 degrees, the rms amounts to $(18.2 \pm 1.4)\%$ for the 360° orbit and to $(17.3 \pm 1.3)\%$ for the 180° orbit. 3D maximum activity projections at regularly spaced angles of the reconstructed Picker's thyroid phantom are presented in Fig. 3.

Typical OS-EM reconstructed slices obtained from the patient PH and UHR SPECT are displayed in Figs 4 and 5 for the parathyroid and shoulder explorations respectively.

DISCUSSION

The 6 mm FWHM measured for a 360° orbit without tilt and PR equal to 10 mm (table 1) compares favourably with the 6.4 mm FWHM obtained with identical equipments excepting a smaller pinhole height of 165 mm [9]. Results in table 1 show that the relative error to the true line distance is less than 6 % for a 180° orbit with or without tilt.

For both the uniformity and Picker's thyroid phantoms, the mean count numbers per pixel were much higher than the mean count numbers that could be obtained in the patient studies. Moreover, because any defects of uniformity or geometry would be more prominent at higher resolution, PH SPECT of the Picker's thyroid was performed with the 3 mm pinhole aperture and the smallest orbit (PR = 75 mm) which could be used for all patients examined by PH SPECT up to now. The uniformity of the reconstructed images of these phantoms is satisfactory (Figs 2 and 3) excepting some non-uniformity and geometric distortions (arrows in Fig 2) in the area opposed to the center of the 180° orbit. This problem can be avoided if the target area is located inside the half cylinder delimited by the rotation orbit and the plane passing through the orbit extremities (Fig 1b) as it has been done for all other PH SPECT data reported in this work. Therefore, the absence of other uniformity artifacts guarantees the absence of such artifacts in the patient studies.

The data sufficiency condition of Tuy [5, 9] is not met for a 180° PH orbit. Moreover, we used only 32 projections for the 180° orbit. This is less than required for optimal sampling but finally turns out to be a good practical compromise with the requirement to minimize the number of camera head rotations. This is a crucial point because it could be observed that most of the patients were very impressed by the rotation of the pinhole close to their body. Anyway, we did not observe the streak

artifacts that could have been generated this angular undersampling and the PH OS-EM reconstruction delivers high quality images : no streak artifact is observed, the uniformity is good, geometry and physical dimensions of the objects are reproduced and the resolution is better than with the parallel hole collimators. Others have also adopted the strategy of 32 projections over 180° and do not report artifacts using an algebraic regularized 3D reconstruction method [10]. In contrast, the FBP approach tends to generate streak artifacts and sagittal slices of poor clinical value [9].

The first clinical study concerned an abnormal parathyroid gland localization using the single tracer ^{99m}Tc -MIBI method. No focal uptake with slower washout kinetics suggesting the presence of an abnormal parathyroid gland was observed on planar images or on the 180° UHR SPECT reconstructed slices (Fig 4 c). In contrast, 180° PH SPECT permits the visualization of 2 focal hyperactivities (Fig 4 a and b): the first one at the posterior border of the median third of the left thyroid lobe (open arrow head), the other one approximately 1 cm behind the basis of the right thyroid lobe (full arrow). The latter focus is also visible on some right anterior oblique projections (Fig 4 d). A better trade-off between resolution and noise is the major improvement allowed by pinhole SPECT as we can notice that a diffuse and low contrast uptake is also detectable in the same regions on the UHR SPECT (Fig 4 c). The presence of an abnormal parathyroid gland could not be validated because the patient was not operated on.

The second patient exploration was a bone scan of the left humeral head. The cortical bone lesions were better defined on the PH SPECT slices (Fig 5) and were confirmed by MRI. Acromio-clavicular articulation and acromial spine were also better seen on PH SPECT. To our knowledge, we report here the first shoulder PH SPECT. Post-filtered PH SPECT slices (Fig 5b) show the degradation of resolution

and contrast due to a resolution loss generated by a gaussian filtering with a 8 mm FWHM, a value representative of the best FWHM that could be expected for UHR SPECT.

The comparison of PH SPECT and UHR SPECT reconstructed slices (Figs 4 and 5) demonstrates a superiority of PH SPECT over UHR SPECT in terms of resolution and overall image quality both for the parathyroid and the shoulder explorations. One should stress the advantage afforded by the tilt which allows to decrease the distance between the pinhole aperture and the neck by more than 50 mm in most cases [2, 10]. A recent study has reported the clinical benefit from the use of PH SPECT in parathyroid explorations [4]. However, the reconstructions were performed using the Feldkamp algorithm (FBP technique) that has been shown to be inferior to OS-EM for PH SPECT reconstruction [9].

CONCLUSION

OS-EM reconstruction of pinhole SPECT for acquisitions with a tilted detector head and only 180° orbit has been shown feasible. On the reconstructed images of line, uniformity and Picker's thyroid phantoms, the geometry, the physical size and the uniformity of the radioactive objects are preserved. A parathyroid exploration and a shoulder bone study have highlighted in a clinical context the gain in resolution associated with the use of the pinhole collimator instead of a parallel hole collimator. This allows a better anatomical localization and the detection of small or complex lesions, a frequent problem encountered by the nuclear medicine physician in the clinical practice. PH SPECT for humans requires only a camera with a very stable center of rotation. Following our experience, the use of the tilt could need some software or hardware adaptations. Some constructors offer a FBP based reconstruction software. Our PH OS-EM software has been implemented in the SMV Vision package.

REFERENCES

1. Jaszczak RJ, Li J, Wang H, Zalutsky MR, Coleman RE. Pinhole collimation for ultra-high-resolution, small-field-of-view SPECT. *Phys Med Biol* 1994; 39: 425-437.
2. Wanet PM, Sand A, Abramovici J. Physical and clinical evaluation of high-resolution thyroid pinhole tomography. *J Nucl Med* 1996; 37: 2017-2020.
3. Bahk YW, Chung SK, Park YH, Kim SH, Lee HK. Pinhole SPECT imaging in normal and morbid ankles. *J Nucl Med* 1998; 39: 130-139.
4. Gabriel M, Erler H, Profanter C, Moncayo R, Riccabona G. Evaluation of parathyroid nodules with thallium/technetium pinhole SPECT. *Eur J Nucl Med* 2000; 27: 1070.
5. Grangeat P, Sire P, Guillemaud R, La V. Indirect cone-beam three-dimensional reconstruction. In: Roux C, Coatrieux JL, eds. *Contemporary Perspectives in Three-dimensional Biomedical Imaging*. Amsterdam: IOS Press; 1997: 29-52 & 343-350.
6. Palmer J, Wollmer P. Pinhole emission computed tomography: method and experimental evaluation. *Phys Med Biol* 1990; 21: 339-350.
7. Li J, Jaszczak RJ, Greer KL, Coleman RE. A filtered-backprojection algorithm for pin-hole SPECT with a displaced center of rotation. *Phys Med Biol* 1994; 39: 165-176.
8. Weber DA, Ivanovic M. Ultra-high-resolution imaging of small animals: implications for preclinical and research studies. *J Nucl Cardiol* 1999; 6: 332-344.
9. Vanhove C, Defrise M, Franken PR, Everaert H, Deconinck F, Bossuyt A. Interest of the ordered expectation maximisation (OS-EM) algorithm in pinhole

- single-photon emission tomography reconstruction : a phantom study. *Eur J Nucl Med* 2000; 27: 140-146.
10. Desvignes P, Laurette I, Koulibaly PM, Migneco O, Bussière F, Darcourt J. An algebraic 3D reconstruction method for pinhole SPECT: validation for cold thyroid nodule detection. *Eur J Nucl Med* 2000; 27: 942.
11. Scarfone C, Jaszczak RJ, Li J, Soo MS, Smith MF, Greer KL, Coleman RE. Breast tumor imaging using incomplete circular orbit PH SPET: a phantom study. *Nucl Med Comm* 1997; 18: 1077-1086.
12. Hudson HM, Larkin RS. Accelerated reconstruction of projection data using ordered subsets of projection data. *IEEE Trans Med Imag* 1994; 13:601-609.

TABLE 1. Full-width at half-maximum and distance between the line sources measured on the reconstructed transverse slices, for 360° or 180 ° orbit and for pinhole aperture of 5 mm.

Pinhole Radius (mm)	Detector Radius (mm)	Tilt Angle (degree)	On-axis FWHM (mm)	Off-axis FWHM (mm)	Distance between lines (mm)
608	270	0	4.90±0.25	4.90±0.25	22.05±0.25 (-5.0%)*
734	270	20	4.90±0.25	5.00±0.25	22.25±0.25 (-4.5%)*
110	3192	0	6.00±0.25	6.05±0.25	21.90±0.25 (-5.6%)*
110	3066	20	5.45±0.25	5.55±0.25	22.25±0.25 (-4.5%)*

* Relative error to the true distance (23.3 mm).

FIGURE CAPTIONS.

FIGURE 1. PH SPECT. (a) detector geometry and orbit parameters. (b) half cylinder delimited by the rotation orbit and the plane passing through the 180° orbit extremities ("best sampled volume", see text for details).

FIGURE 2. Transverse slices from the half upper, center and half lower regions of the uniformity phantom for a 360° or a 180° orbit and with 0° or 20 tilt angle (PH SPECT). Pinhole aperture was 5 mm.

FIGURE 3. 3D maximum activity projections of the reconstructed Picker's thyroid phantom for a 180° orbit and 0° or 20 tilt angle (PH SPECT). Pinhole aperture was 3 mm.

FIGURE 4. Patient suffering from hyperparathyroidism. Coronal slices of the thyroid area from the OS-EM reconstruction of (a) PH SPECT, (b) PH SPECT and 5.4 mm FWHM gaussian post-filtering (value in the range of the FWHMs measured (Table 1) for PH SPECT and the orbit used), (c) UHR SPECT. Slice thickness is 2.0 mm and slice pixel size is 1.0 mm. Two focal hyperactivities are detected: the first one at the posterior border of the median third of the left thyroid lobe (open arrow head), the other one approximately 1 cm behind the basis of the right thyroid lobe (full arrow). (d) After inspection of the PH reconstructed slices, a low tracer uptake (arrows) could also be observed in some PH SPECT right anterior oblique projections. Pinhole aperture was 5 mm.

FIGURE 5. Shoulder bone SPECT exploration. Coronal slices from the OS-EM reconstruction of (a) PH SPECT, (b) PH SPECT and 8.15 mm FWHM gaussian post-filtering (value close to the best FWHM that could be expected from UHR SPECT), (c) UHR SPECT. Slice thickness is 5.6 mm and slice pixel size is 2.8 mm.

Tomography demonstrated lesions of the cortical bone that outline the left humeral

Post-print author

head circumference with a more pronounced hyperactivity in its posterior part. These lesions were better defined on PH SPECT and were confirmed by MRI. Pinhole aperture was 5 mm.

FIGURES

Figure 1

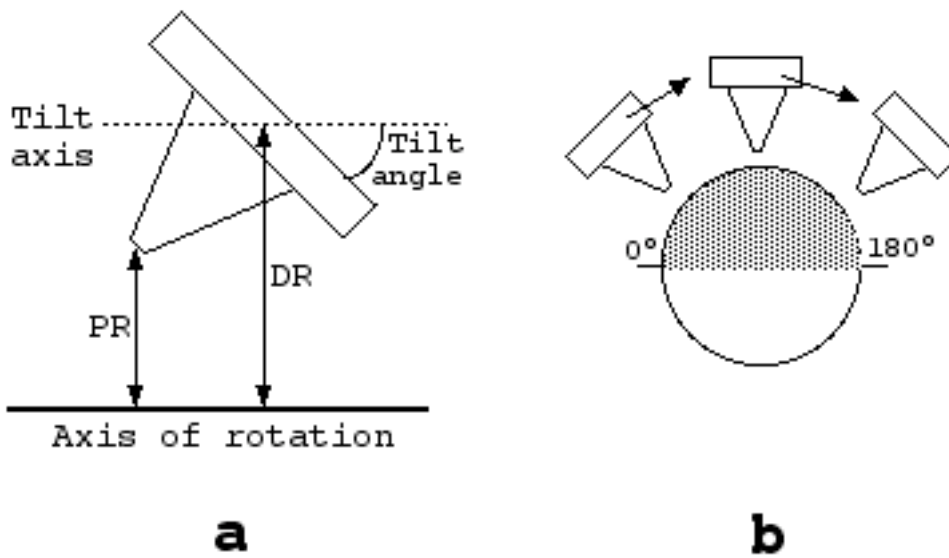


Figure 2

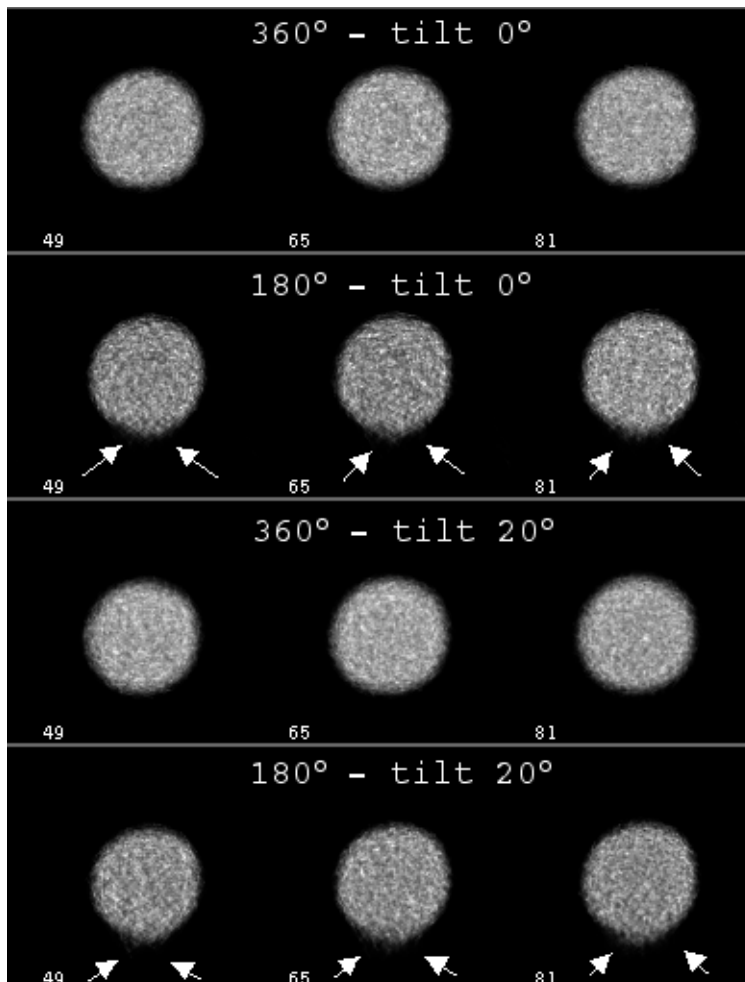


Figure 3

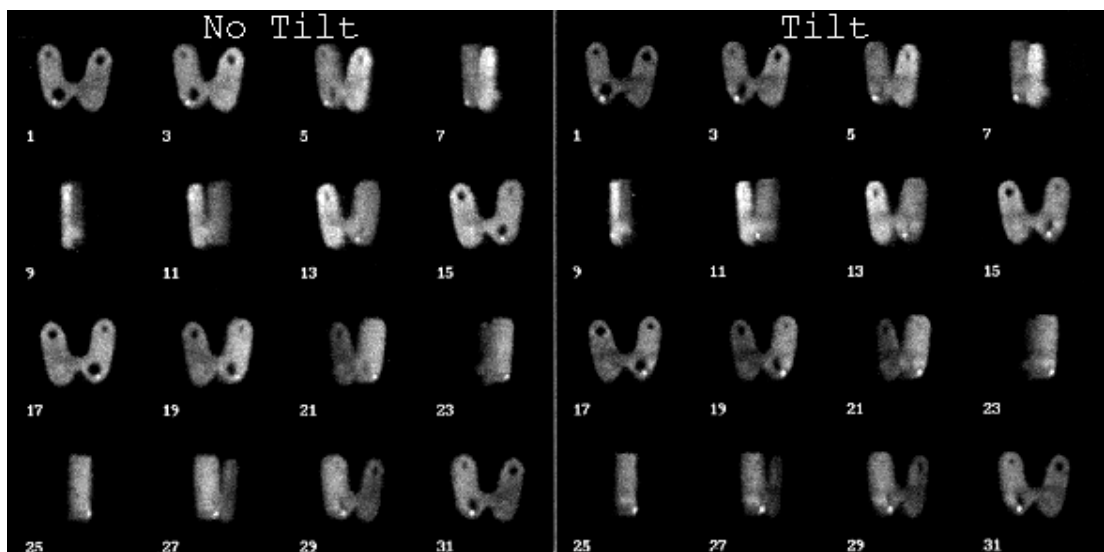


Figure 4

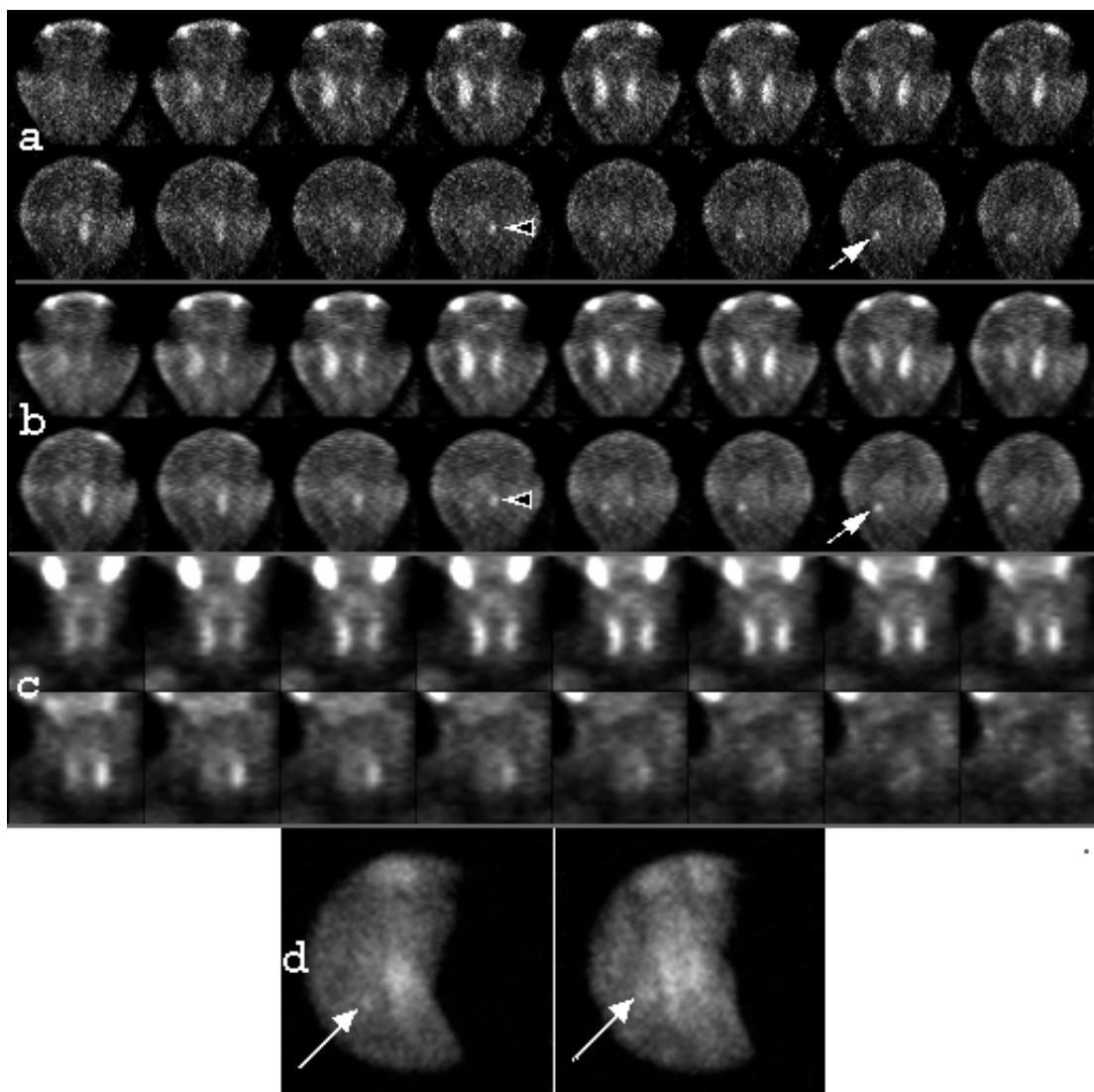


Figure 5

